JOURNAL OF AGRICULTURAL AND FOOD CHEMISTRY
ARTICLE

J. Agric. Food Chem. **2009,** *57,* 5853–5864 **5853**
DOI:10.1021/jf900870j

New Chemical Clues for Broomrape-Sunflower Host−Parasite Interactions: Synthesis of Guaianestrigolactones

Francisco A. Macías,*,† María D. García-Díaz,† Alejandro Pérez-de-Luque,‡ Diego Rubiales,§ and Juan C. G. Galindo†

†Grupo de Alelopatía, Depto. de Química Orgánica, Facultad de Ciencias, Universidad de Cádiz, Avda. República Saharaui s/n, Apdo. 40, 11510, Puerto Real, Cádiz, Spain, ‡IFAPA-CICE, CIFA "Alameda del Obispo", Apdo. 3092, 14080, Córdoba, Spain, and §Institute of Sustainable Agriculture, IAS-CSIC, 14080, Córdoba, Spain

A comparative structure−activity relationship (SAR) study has been conducted with several guaianolide sesquiterpene lactones (SLs) as inducers of the germination of sunflower broomrape (*Orobanche cumana*) seeds. Compounds were selected and synthesized to study the influence of the lactone−enol−γ-lactone moiety on the selectivity of SLs toward the stimulation of sunflower broomrape germination. The results clearly illustrate that SLs are recognized only by *O. cumana*, while the introduction of a strigol-like second lactone moiety in the guaianolide backbone results in the loss of specificity and hence the germination of other broomrape species. We have named this new class of compounds guaianestrigolactones (GELs).

KEYWORDS: Sesquiterpene lactones; guaianolides; guaianestrigolactones; SAR; germination stimulants; allelopathy; parasitic weeds; broomrape; *Orobanche cumana*; Orobanchaceae

INTRODUCTION

Sunflower (*Helianthus annuus* L.) is an important crop in several parts of the world as it is used as a source of vegetable oil and seeds, and also as a fertilizer. Sunflowers can be parasitized specifically by the root holoparasitic plant *Orobanche cumana*. Sunflower crops are in danger because of severe infestation by this parasite in several million hectares throughout eastern and southern Europe and in Asian countries including China (*1*). The effectiveness of conventional control methods to date is limited because of numerous factors including the complex nature of the parasites, which reproduce by tiny and long-lived seeds that can remain dormant and viable for a period of almost 20 years (*2*), and the difficulty in diagnosis until the crop is irreversibly damaged. The intimate connection between host and parasite also hinders efficient control by herbicides. Once a new episode of broomrape has been documented in an area, this weed spreads rapidly because of the high level of seed production per plant (thousands of seeds) and their small size. Spreading factors, to name the most common ones, include the wind, the soil attached to the tires of agricultural machinery, and the residues of the infested crops.

Some satisfactory results have been found in certain cases by using herbicides such as glyphosate, imidazolinones, or sulfonylureas (*1*, *3*−*6*). Other possible agricultural practices for broomrape control include crop rotation (*7*), intercropping (*8*), use of fertilizers (*9*), breeding (*10*), activators of systemic acquired resistance (*11*) and resistant cultivars (*12*−*14*), and synthetic germination stimulants (*15*).

*Corresponding author. Phone: +34-956-016370. Fax: +34-956-016193. E-mail: famacias@uca.es.

Host−parasite interaction is extremely specific and depends on chemical recognition. Several natural germination inducers have been isolated from their corresponding hosts (*16*). A number of natural products obtained from nonhosts also present germination-inducing activity (*16*). With the exception of sorgoleone, all natural inducers obtained from host plants belong to the so-called strigolactone group of compounds, which have a postulated biogenetic origin in the carotenoids pathway (*17*). These materials have been isolated from sorghum (*18*−*20*), red clover (*21*), and cow pea (*22*). Surprisingly, strigolactones also occur in nonhost species such as cotton (*23*), *Menispermum dauricum*, and *Stephania sepharantha* (*24*), and it has been suggested that they might occur widely in the plant kingdom. Host recognition might be the result of a coevolution process by which the parasite takes advantage of and recognizes certain chemicals exuded by the host plant for other purposes (mainly defense, excretion, or mycorrhyzation (*25*, *26*)). These chemicals are detected by the parasite as an indication of a viable host nearby and trigger the cascade of events that lead to germination. Environmental factors such as humidity and temperature are crucial for a positive germination response (*27*). During the conditioning period, changes occur inside the seed and prepare it for the detection of a chemical signal. This period is water- and temperature-dependent (*28*, *29*), and such restrictions are supposed to ensure germination in the best conditions for both the parasite and the host. In the search for healthy plants to attach to, the healthier the host the greater the probability for the successful development of the parasite.

To our knowledge, the specific germination stimulants of sunflower broomrape remain unknown. However, our previous work with SLs shows that these compounds are specific inducers

 Published on Web 06/09/2009

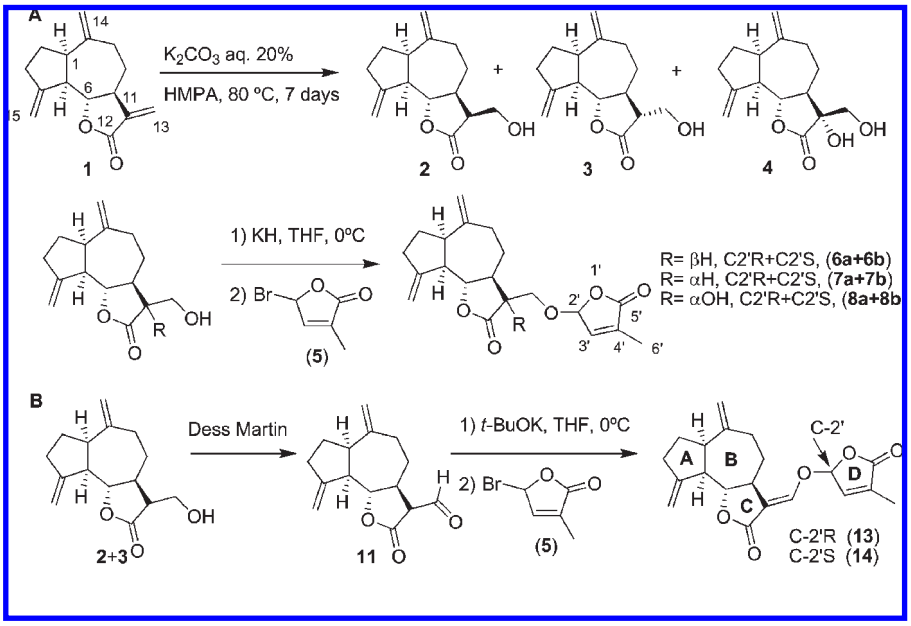

Figure 1. (**A**) Synthetic procedure followed to obtain strigolactone-like SLs (GELs). The numbering in the second lactone ring has been assigned according to the latest accepted convention followed for strigolactones (*34*). (**B**) Synthetic pathway to obtain GELs.

of *O. cumana* and do not induce a germination response in other *Orobanche* species (*30*, *31*). The main objective of the work described here was to determine whether sunflower broomrape is able to recognize the lactone ring present in SLs or if this specificity is lost when a lactone−enol−γ-lactone system similar to that of strigolactones is introduced into the SL backbone. We have named such compounds guaianestrigolactones. If such a hypothesis is confirmed, then the lactone ring alone could be identified as the specific bioactiphore of SLs for sunflower broomrape.

MATERIALS AND METHODS

General Considerations and Starting Material. The main objective was to verify whether the introduction of an enol-γ-lactone-like moiety into the SL would induce any change in the bioactivity and the selectivity toward the germination of the different broomrape species. For this study, the guaianolide backbone was selected as a case study on the basis of our previous results with several other SL types (*30*, *31*) and because of the availability of dehydrocostuslactone (**1**) in multigram amounts to serve as the starting material. Pure material was obtained from the commercial root extract of *Saussurea lappa* (Costus Resin Oil, Pierre Chauvet, S.A.) by column chromatography on silica gel (Hx/AcOEt 5%) and purified by recrystallization from Hx/Et_2O mixtures along with the other major compound costunolide. The spectroscopic (^1H and ^{13}C NMR and HRMS) and physical data (m.p.) were fully consistent with those reported in the literature (*32*, *33*).

Synthesis of 11,13-Dihydroguaianestrigolactones (11,13-dihydroGELs). In order to assess the importance in the germination activity of the second lactone ring alone, i.e., without the enol moiety, compounds were synthesized in two steps according to the synthetic route depicted in **Figure 1**. The numbering for ring D is assigned according to the latest accepted convention for strigolactones (*34*).

Michael addition of the hydroxy group was performed according to the methodology developed by our group (*35*), and this yielded the mono- and dihydroxylated derivatives **2** (21%), **3** (30%) and **4** (6%), with some starting material **1** remaining (30%).

2-Methyl-4-bromobut-2-ene-1,4-olide (**5**) was generated by treatment of the corresponding 2-methylbut-2-ene-1,4-olide (Sigma-Aldrich, Co.) with NBS in CCl_4 solution and a catalytic amount of benzoylperoxide as a radical initiator (*36*). The reaction mixture was heated under reflux at 78 °C for 1.5 h to give **5** in almost quantitative yield. The compound obtained was the racemic mixture of epimers at C-4′. Because of the low stability of this compound, it is strongly recommended to be immediately used for the nucleophilic substitution step.

Treatment of **3** with potassium hydride under an argon atmosphere in dry THF (0 °C) yielded the corresponding alkoxide at C-13, and this was followed by the addition of an excess of bromolactone **5** dissolved in dry THF. The reaction mixture was allowed to react for 7 h at room temperature, after which further evolution was not observed by TLC. The SN_2 substitution on the bromine atom yielded the mixture of diastereomers **6(a+b)** (13%) and **7(a+b)** (4%), with starting material recovered (60%) and traces of the elimination product **1** detected. A similar procedure was followed using **4** as the starting material, and this gave rise to the diastereomeric mixture **8(a+b)** (7.5%) with 60% of the starting material recovered. All attempts to separate the two diastereomers present in each mixture by chromatographic means including chiral phase HPLC columns were unsuccessful.

Synthesis of Guaianestrigolactones (GELs). 13-Hydroxycostuslactone (**2**) and 13-hydroxy-*epi*-costuslactone (**3**) (or their mixture) were oxidized to the corresponding aldehydes (**11**) using the Dess−Martin periodinane reagent (57% yield). The introduction of the second lactone ring D was achieved using a procedure (dry THF, 0 °C, base 1 equiv) similar to that used for dihydro-GELs. Thus, enolate **12** was generated using potassium *tert*-butoxide (*t*-BuOK) as this gave better yields than potassium hydride. Once enolate **12** was added, it smoothly underwent SN2 displacement of the bromine atom in racemic bromolactone **5** (**Figure 1**) to yield a mixture of **13** and **14** in 42% global yield. C-11(*S*) (**2**), C-11(*R*) (**3**) hydroxycostuslactone, or a mixture of the two can be used as starting material for the synthesis of guaianestrigolactones as the stereospecificity at C-11 is lost after the formation of the enolate. In this case, the racemic mixture of the diastereoismers at C-2′ (**13** and **14**) could be separated by HPLC (silica gel, Lichrospher Column and Hx/AcOEt 4:1 as eluant), and the compounds were characterized spectroscopically.

Bioassays. *Orobanche spp. Germination Bioassays.* Two populations of *O. cumana*, denoted 12 and 23, with different degrees of virulence were collected from experimental sunflower infected fields by Dr. González Carrascosa (Semillas Cargill, Spain). Seeds of *O. ramosa* were provided by Dr. D. M. Joel (Department of Weed Research, Agricultural Research Organization, Newe-Ya'ar Research Center, Israel). The *Orobanche* germination bioassay on filter paper was performed as previously reported (*30*, *37*). Compounds were tested at 10, 1, 0.1, and 0.01 μM aq soln (0.1% acetone as cosolvent). Seeds were preconditioned in darkness (24 °C, 11 days, and 0.3 mM MES (2-[*N*-morpholino]-ethanesulfonic) acid buffer; pH was adjusted to 6 with 0.1 M NaOH) and germinated in the presence of the test compound (darkness, 24 °C, 6 days). A parallel treatment with 10 μM GR-24 was set up as an internal positive control. Germination was observed

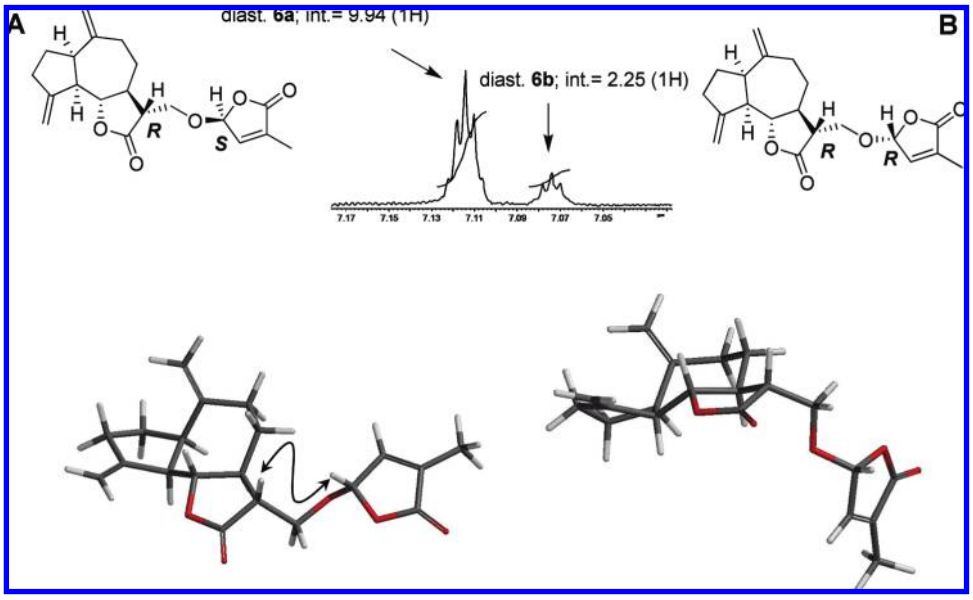

Figure 2. (**A**) Main diagnostic NOE effect observed is depicted in the only local minimum that allows such an effect (2% of the total conformer population) in the diastereomer (11*R*,2′*S*). (**B**) Minimum energy conformer (84% of the total population) in the diastereomer (11*R*,2′*R*); none of the local minima were able to give any NOE effect. Conformer distributions were obtained using the Montecarlo MMFF force field (Spartan'06).

under a dissection microscope (30×) starting on the third day after the addition of the compound. Seeds were considered to be germinated when the radicle was at least 0.2 mm long. Germination was expressed as a percentage of the total seeds.

Stock solutions were prepared with acetone and diluted with 0.3 mM MES to obtain a 10 μM (0.1% acetone) solution; test solutions at 1, 0.1, and 0.01 μM were prepared by diluting with 0.3 mM MES (0.1% acetone aq solns).

Molecular Modeling. Molecular calculations were performed using Spartan'06, PCModel 7.50.00 (Serena Software), and Chem3D Ultra 7.5. Spartan'06, PCModel 7.50.00, and Chem3D Ultra 7.5 were used to obtain local minimum energy structures using semiempirical PM3 and AM1 calculations. Conformer distribution (Spartan'06) was obtained using the Montecarlo program with the MMFF force field; MAXCONFS were set to 1000, which proved to be sufficient as none of the calculations yielded more than 100 conformers. Single point Hartree−Fock (3-21G(*)) calculations were performed in some cases to refine the values obtained for the heat of formation (*38*). For transition state calculations, a first approach to the geometry was obtained using semiempirical calculations (PM3; keywords, transition state geometry; geometrycycle = 10000), and the resulting geometry was then refined using ab initio calculations (restricted Hartree−Fock using the basis set 3-21G(*)). The energy values were then refined using electron density correlation methods (B3LYP using the basis set 6-21G(*), keywords, single point energy; geometrycycle = 10000).

Chem3D Ultra 7.5 was used in some cases to obtain a fast approach to basic minimum energy structures but not for transition state calculations. The GMMX command was then used to generate other low energy local minima. These conformers were further minimized using PM3 calculations (MOPAC) (*39*) to obtain more accurate theoretical $\Delta H°_f$ searching for the real minimum energy conformer. The local minima obtained were compared with those obtained from Spartan'06. Usually, geometries obtained from Chem3D and Spartan'06 were similar or identical. In cases where a significant difference arose, refined ab initio calculations using Spartan'06 allowed the geometry to be chosen on the basis of more accurate enthalpies of formation. Volume, height, and energies of the molecular orbitals were obtained from PCModel (MOPAC) and Spartan'06.

RESULTS AND DISCUSSION

Spectroscopic Characterization: DihydroGELs. The mixture of diastereomers (**6a** + **6b**) presents a molecular ion in the HRMS at *m*/*z* 344.1601, which is consistent with the molecular formula $C_{20}O_5H_{24}$. The incorporation of the lactone moiety is further confirmed by the new signals appearing in the ^{1}H NMR spectrum at δ 5.11 (1H, *m*, H-2′) and δ 1.91 (3H, *dd*, H-6′), which correspond to the hemiketal proton and the methyl group present in the new lactone ring, respectively. The ^{13}C NMR spectrum also contains new signals corresponding to the lactone moiety (carbons C2′ to C6′; **Table 2**). The two signals obtained for the vinyl proton at δ 7.07 (0.19H, *m*, H-3′a) and δ 7.11 (0.81H, *m*, H-3′b) evidence the racemic nature of the mixture, with each corresponding to a different enantiomer at C-2′. Signal duplicity is also observed in the ^{13}C NMR spectrum, and each set of signals was unequivocally correlated through ^{1}H-^{13}C g-HSQC and ^{1}H-^{13}C g-HMBC heteronuclear correlation experiments. The connection between the guaianolide backbone and the new lactone ring is confirmed through the ^{1}H-^{1}H NOESY experiment as a correlation between the signals corresponding to H-11 and H-2′ can be observed, corresponding to the NOE effect between these two protons (**Figure 2**). The integral ratio (9.94:2.25, **6a**/**6b**) also establishes relative yields for each diastereomer as 82% (**6a**) and 18% (**6b**) (d.e. = 64%) for the total mixture (**Figure 2**).

The absolute stereochemistry of each diastereomer was unequivocally established through NOESY experiments: a positive NOE effect was observed between the proton signals of H-11 and H-2′ in the major diastereomer (**6a**). A conformational search on both C-2′R and C-2′S diastereomers concluded that major minimum energy conformers, accounting for 84% and 71% of the total conformer population, were not able to present any NOE effect because of the opposite disposition of these protons. However, while none of the local minima obtained for the C-2′R diastereomer were able to present NOE effects between H-11 and H-2′, a local minimum with the appropriate spatial disposition accounting for 2% of the conformer population was found in the C-2′S diastereomer. Consequently, an absolute configuration (11*R*,2′*S*) can be established for **6a**, while the minor diastereomer has the (11*R*,2′*R*) configuration (**Figure 2**).

Not surprisingly, treatment of **3** also led to a small amount of the mixture (**7a** + **7b**), and this had spectroscopic properties similar to those of mixture (**6a** + **6b**) (**Tables 1** and **2**) but without any diastereomeric excess, as shown by the relative intensities of the integrals obtained for H-2′ and H-3′ (**7a**/**7b,** 1:1, d.e. = 0) and the value of $[\alpha]^{25}_D = +0.0$. Extensive NOE and NOESY studies

Table 1. ^{1}H NMR Chemical Shifts of **6**−**11**, **13**, and **14**[a]

H	6a/6b	7a/7b	8a/8b	9	10	11	13	14
1	2.89 *ddd*	2.87	2.87	2.89 *m*	2.90 *ddd*	2.93 *m*	2.89 *ddd*	2.89
2α	1.85 *dddd*	1.86	1.82[a]	1.82	1.83 *dddd*	1.87 *m*	1.87	1.87
2β	1.93 *m*	1.94	1.94[a]	1.97*dddd*	1.97	1.94 *m*	1.87	1.87
3α	2.53 *m*	2.45[a]	2.50[b]	2.51	2.48	2.50	2.50	2.51
3β	2.15 *m*	2.17[a]*m*	2.02[b]	2.51	2.48	2.50	2.50	2.51
5	2.80 *dd*	2.83	2.81	2.89	3.14	2.82	2.77	2.78
6	3.97 *dd*	3.95	4.04/3.99	4.15	4.23	4.03	3.98	3.97
7	2.23 *m*	2.41	2.46	2.56 *ddd*	3.28	2.72 *dddd*	3.01	3.03
8α	2.26 *dddd*	2.15 *m*	2.08	2.18	2.15 *dddd*	2.17	2.50	2.54
8β	1.31 *dddd*	1.31	1.42	1.44	1.50	1.32	1.40	1.40
9α		2.05[b]	2.08[c]	2.02	2.54		2.12*ddd*	2.13*m*
9β		2.42[b]	1.98[c]	2.51	2.02		2.38*ddd*	2.3
11	2.04 *brdd*	2.41 *m*				3.26*d*		
13	3.94 *dd* (2H)	3.85 *dd*/4.07 *brs*	4.05/3.79 *d*	4.48	4.76	9.88	7.43	7.43
13′		3.97	3.70/3.73 *d*	4.37	4.66			
14	4.86 *brs*	4.87	4.89/4.87 *s*	4.87	4.82	4.89*brs*	4.86*s*	4.86
14′	4.77 *brs*	4.77	4.79/4.76 *s*	4.77	4.74	4.79*dd*	4.80*s*	4.80
15	5.16 *brdd*	5.18	5.18/5.15	5.20 *brd*	5.33	5.17*d*	5.25	5.25
15′	5.04 *brdd*	5.04*brd*	5.06/5.07 *dd*	5.07 *brd*	5.11	5.05*d*	5.05	5.04
2′	5.11 (a) *ddq*/ 5.46 (b) *dq*	5.89/5.83	5.80/5.71				6.08*dq*	6.09
3′	7.11(a) /7.07 (b) *dq*	6.85/6.80	6.77	7.99*brt* (2H)	7.99		6.91*dq*	6.90
4′				7.43 *dd* (2H)	7.58			
5′				7.57 *tt*	7.46			
6′	1.91(a) *dd*	1.94/1.96	1.95/1.93	7.43 *dd* (2H)	7.58		2.02	2.02
7′				7.99*brt* (2H)	7.99			
3″					8.04 *dd*			
4″					7.60 *dd*			
5″					7.43 *dd*			
6″					7.60 *dd*			
7″					8.04 *dd*			

[a] 600 and 400 MHz, $CDCl_3$, signal of residual $CHCl_3$ centered at δ 7.25 ppm. [a,b,c] Superscripts within the same column: these signals may be interchanged.

Table 2. ^{13}C NMR Chemical Shifts of **6**−**11**, **13**, and **14**[a]

C	6	7	8	9	10	11	13	14
1	47.1 *d*	46.9/47.0	47.04/46.7	47.1	47.1	47.1	48.0	47.9
2	30.1 *t*	30.2	30.1/29.7	27.4	27.6	30.2	30.3	30.3
3	32.5[a]*d*	32.5/32.6	32.5	32.7	32.9	32.6	32.5	32.5
4	151.5 *s*	151.6/151.7	151.39/151.33	151.6	151.9	151.3	151.0	151.5
5	51.8 *d*	51.7/51.8	52.5	52.6	52.6	51.7	51.9	51.9
6	85.5 *d*	85.6/85.7	83.8/83.6	83.8	84.5	86.1	85.1	85.2
7	43.2 *d*	47.7/48.1	51.0/50.9	51.5	46.5		43.5	43.4
8	32.2[a]*t*	32.4	26.9/26.7	31.2	30.3		29.6	29.8
9	37.2 *t*	37.5/37.7	37.2/37.1	37.7	37.6	37.3	35.4	35.7
10	149.6 *s*	149.8	149.6/149.5	149.9	149.2	149.3	149.0	149.0
11	31.7 *d*	43.3/44.6	76.1/75.8 *s*	76.1	80.6		112.2	112.0
12	177.2 *s*	175.4	177.2	176.6	172.0	177.8	171.4	171.3
13	85.5 *t*	64.6 (a)/ 66.1 (b)	70.4/68.2	65.0	63.5	195.2	150.5 *d*	150.4
14	112.1/112.2 *t*	111.95/112.0	112.3	112.6	112.4	112.4	112.8	112.7
15	109.3 *t*	109.1/109.2	109.63/109.56	109.8	109.3	109.4	109.8	109.7
1′				166.2 *s*	165.4			
2′	78.3 (a)/78.6(b) *d*	101.1 (a)/102.0 (b)	101.2/100.6	129.3 *s*	128.85		100.7 *d*	100.6
3′	148.4 (a) /148.6 (b) *d*	142.7/142.8	142.14/142.09	130.1	130.0		140.9	140.7
4′	130.5 *s*	134.1/134.7	135.1/134.6	128.9 *d*	128.63		135.9	136.1
5′	173.8 *s*	171.7/171.8	171.1	133.9 *d*	133.9		170.2	170.2
6′	10.6 *q*	10.60/10.64	10.6	128.9 *d*	128.63		10.8	10.8
7′				130.1 *d*	130.0			
1″					164.6 *s*			
2″					128.77 *s*			
3″					129.8 *d*			
4″					128.60 *d*			
5″					133.6 *d*			
6″					128.60 *d*			
7″					129.8 *d*			

[a] 100.6 and 50.3 MHz, $CDCl_3$, signal of residual $CHCl_3$ centered at δ 77.0 ppm. Degree of protonation and assignments were established by APT, HETCOR, and HSQC experiments; multiplicities are not repeated if identical with those in the preceding column. [a,b,c] Superscripts within the same column: these signals may be interchanged.

did not show any signal of diagnostic importance to assign the absolute configuration of each diastereomer. The formation of this mixture is explained through base-catalyzed epimerization at C11 of the starting material, as this has an acidic proton in this position. The higher yield obtained for the mixture with an (11*R*) configuration (**6a** + **6b**) is in good agreement with our previous results concerning the relative stability of the two epimers (**2** and **3**) when obtained by a Michael addition of a hydroxy group to the dehdyrocostuslactone (**1**) (*35*).

Finally, treatment of **4** under the same conditions yielded the mixture of diastereomers **8a** and **8b**, again as an equimolecular mixture. As discussed previously, the introduction of the new lactone ring was confirmed by HRMS, which gave a molecular ion at *m*/*z* 360.1543, consistent with a molecular formula $C_{20}O_6H_{24}$. The ^{1}H NMR spectrum presented major diagnostic signals at δ 6.77 (2H, *m*, H-3′), corresponding to the vinyl proton at ring D in both diastereomers, and differentiated signals for the methyl group and the H-2′ proton in each diastereomer (δ 1.93 3H, *dd*, H-6′b; δ 1.95 3H, *dd*, H-6′a; δ 5.71 1H, *dd*, H-2′b; δ 5.80 1H, *dd*, H-2′a). The integral ratio for each pair of signals was 1:1, which established their relative proportions as 1:1. The incorporation of the lactone ring into the guaianolide backbone was further substantiated in the ^{13}C NMR spectrum by the presence of new signals at δ 171.1 (C-5′, lactone group), δ 142.1 (C-3′, vinyl carbon), and δ 10.6 (C-6′, methyl group). Once again, each diastereomer presented differentiated chemical shifts for carbon C-2′ (δ 100.6, C-2′a; δ 101.2, C-2′b). Surprisingly, differentiated signals can also be observed for H-13, H-13′, H-6, C-13, and C-6 (**Tables 1** and **2**). Signals for each diastereomer were assigned by using homo- and heteronuclear correlation experiments (^{1}H-^{1}H COSY and ^{1}H-^{13}C gHMQC), but the absolute configuration at C-2′ could not be elucidated.

Molecular modeling of the transition state (B3LYP using the basic set 6-31-G*) shows a difference in energy of −0.08444 hartree (−52.986 kcal/mol) between the C2′S and C2′R transition state in favor of the C2′S diastereoisomer in the case of **6**. Such a difference was not observed when the calculations were carried out with the transition state that yields **7** (see Supporting Information). These results are in good agreement with the diastereomeric excess obtained in the case of **6**. The spatial requirements of the methyl group in the lactone ring D could be responsible for the observed effect as it forces the orientation of this ring in the transition state to minimize the steric hindrance. The α orientation of this moiety in **6** makes the steric hindrance higher in the transition state of the C2′R diastereomer, while the β orientation causes this moiety to lie away from the rest of the molecule in **7**. Consequently, the methyl group does not influence the orientation, and the differences in steric hindrance between the two possible diastereomers are minimized (a more detailed discussion on the theoretical data is carried out in the Supporting Information section).

Elimination of the hydroxyl group under strong basic conditions can compete with the generation of the alkoxyde; in compounds **2** and **3**, the acidic proton H-11 easily undergoes elimination toward **1**, while the same reaction with the tertiary hydroxyl group at C-11 in **4** will lead to the aldehyde **11**. All attempts to increase the yield of the alkoxyde varying the type and amount of base used resulted in the increase of **1** and **11**. Only under the conditions described was it possible to obtain the compounds resulting from the coupling of the alkoxyde and the bromo-lactones **6**−**8** without detecting the elimination products **1** and **11**.

Benzoylperoxide can compete with the nucleophilic substitution of the alkoxide if the reaction mixture is not carefully filtered. If such a competitive process occurs, the compounds resulting from the addition of the benzoyl moiety, **9** (10%) and **10** (6%), can be isolated. Compound **9** gave rise to a molecular ion in the HRMS at *m*/*z* 368.1618, corresponding to the molecular formula $C_{22}O_5H_{24}$. The major diagnostic signals in the ^{1}H NMR spectrum were those corresponding to the aromatic ring at δ 7.43 (2H, *dd*, H-4′), δ 7.57 (1H, *dd*, H-5′), and δ 7.99 (2H, *dd*, H-3′). This was further substantiated by the ^{13}C NMR spectrum, which contained signals corresponding to the carbon ester at δ 166.2 (C-1′) and the aromatic ring (one quaternary carbon, one methyne carbon, and two equivalent methyne carbons; **Table 2**).

Compound **10** gave a molecular ion in the HRMS at *m*/*z* 472.1889, corresponding to the molecular formula $C_{29}O_6H_{28}$, and the main fragmentation products at *m*/*z* 350.1533 ([M − PhCOOH]$^+$) and 228.1146 ([M − 2PhCOOH]$^+$). Evidence for the incorporation of two benzoyl ester groups could also be observed in the ^{1}H NMR spectrum as two independent sets of aromatic signals, as clearly established through the ^{1}H-^{1}H COSY experiment. As these compounds represent an interesting modification of the primary skeleton to investigate the effect of increasing volume and steric requirements in the vicinity of the reactive center on the germination activity, they were also used in the bioassays.

(6*R*),(7S),(11*R*)-13-[4′-Methyl-3′-ene-2′-oxy-γ-butyrolactone]-4(15),10(14)-diene-guaiane-6α,12-olide (mixture of **6a** and **6b**; d.e. = 64%) was obtained as a colorless oil; $[\alpha]^{25}_D$ + 5.6 (*c* 0.04, $CHCl_3$); IR (neat, KBr) ν_{max} 2963, 2924, 2851 (C−H), 1760, 1730 (C═O, γ-lactone) cm^{-1}; ^{1}H NMR (600 MHz): See **Table 1**. *J* (Hz): 1,2α = 8.1; 1,2β = 5.0; 5,6 = 5,1 = 9.2; 6.7 = 9.3; 7,8α = 3.1; 7,8β = 13.2; 8α,8β = 12.1; 8α,9α = 12.1; 8α,9β = 9.4; 8β,9α = 11.1; 8β,9β = 4.8; 11,13 = 11,13′ = 9.4; 3,15 = 5,15 = 2.3; 2′(a), 3′(a) = 3.1; 3′(a),6′(a) = 1.5; 2′(a),6′(a) = 1.8; 2′(b),6′(b) = 4.0. ^{13}C NMR (100 MHz): see **Table 2**. EIMS (70 eV) *m*/*z* (rel. int.): 344 [M]$^+$ (0.5), 328 [M − CH_4]$^+$ (23), 216 [M − CH_4 − CH_3O − C_4O_2H]$^+$ (17), 159 [M − CH_4 − CH_3O − C_4O_2H − CO_2 − CH_3]$^+$ (100); HRMS *m*/*z* 344.1606 (calcd for $C_{20}O_5H_{24}$ 344.1624).

(6*R*),(7*S*),(11*S*)-13-[4′-Methyl-3′-ene-2′-oxy-γ-butyrolactone]-4(15),10(14)-diene-guaiane-6α,12-olide (racemic mixture of **7a** and **7b**) was obtained as a colorless oil; $[\alpha]^{25}_D$ + 0.0 (*c* 0.04, $CHCl_3$); IR (neat, KBr) ν_{max} 2963, 2926, 2856 (C−H), 1770, 1734 (C═O, γ-lactone) cm^{-1}; ^{1}H NMR (600 MHz): see **Table 1**. *J* (Hz): 1,2α = 8.2; 1,2β = 4.2; 1,5 = 9.3; 2α,3α = 4.0; 2α,3β = 6.0; 5,6 = 6,7 = 9.5; 8α,8β = 12.1; 8β,7 = 12.1; 8β,9α = 11.3; 8β,9β = 5.0; 9α,8α = 5.2; 9α,9β = 11.3; 11,13(a) = 3.6; 11,13′(a) = 4.4; 13(a),13′(a) = 10; 1,14 = 1,14′ = 1.3; 3,15 = 5,15 = 3′,15 = 2.2; 2′(a),3′(a) = 1.5; 3′(a), 6′(a) = 1.3; 2′(a),6′(a) = 1.3; 2′(b),3′(b) = 1.3; 3′(b),6′(b) = 1.8; 2′(b),6′(b) = 1.3. ^{13}C NMR (100 MHz): see **Table 2**. EIMS (70 eV) *m*/*z* (rel. int.): 344 [M]$^+$ (0.5), 328 [M−CH_4]$^+$ (23), 216 [M−CH_4− CH_3O− C_4O_2H]$^+$ (17), 159 [M − CH_4 − CH_3O − C_4O_2H − CO_2 − CH_3]$^+$ (100); HRMS *m*/*z* 344.1606 (calcd for $C_{20}O_5H_{24}$ - 344.1624).

(6*R*),(7*S*),(11*R*)-11-Hydroxy-13-[3′-methyl-3′-ene-4′-oxy-γ-butyrolactone]-4(15),10(14)-diene-guaiane-6α,12-olide (racemic mixture of **8a** and **8b**) was obtained as a colorless oil; $[\alpha]^{25}_D$ −3.4 (*c* 0.04, $CHCl_3$); IR (neat, KBr) ν_{max} 3390 (OH, st), 2925, 2853 (C−H), 1789, 1770, (C═O, γ-lactone) cm^{-1}. ^{1}H NMR (600 MHz): see **Table 1**. *J* (Hz): 1,2α = 4.8; 1,2β = 8.1; 1,5 = 16.0; 5,6 = 6,7 = 9.7; 8α,8β = 16.1; 7,8α = 4.5; 8α,9α = 8α,9β = 7.8; 13, 13′(a) = 9.5; 13,13′(b) = 9.7; 3,15(a,b) = 5,15 = 2.1; 3,15′(a) = 5,15′ (a) = 2.3; 2′,3′(a) = 2′,6′(a,b) = 1.4; 3′,6′(a) = 1.6; 3′,6′(b) = 1.4. ^{13}C NMR (100 MHz): see **Table 2**. EIMS (70 eV) *m*/*z* (rel. int.): 360 [M]$^+$ (0.5), 342 [M − H_2O]$^+$ (18), 263 [M − $C_5H_5O_2$]$^+$ (34), 159 (100); HRMS *m*/*z* 360.1543 (calcd for $C_{20}O_6H_{24}$ 360.1573).

(6*R*),(7*S*),(11*R*)-11-Hydroxy-13-benzoyloxy-4(15),10(14)-diene-guaiane-6α,12-olide (**9**) was obtained as an amorphous white solid. ^{1}H NMR (600 MHz): see **Table 1**. *J* (Hz):

1,2α = 6.3; 1,2β = 1.1; 2α, 2β = 13.1; 2α,3α = 8.5; 2α,3β = 4.2; 5,6 = 8.7; 6,7 = 10.0; 7,8α = 3.1; 7,8β = 13.1; 8α,8β = 12.7; 8β,9α = 12.7; 8β,9β = 4.6; 8α,9α = 9.8; 8α,9β = 8.8; 13,13′ = 11.5; 3,15 = 3,15′ = 1.8; 3′,4′ = 8.2; 3′,5′ = 1.5; 4′,5′ = 7.9. ^{13}C NMR (100 MHz): see **Table 2**. EIMS (70 eV) *m*/*z* (rel. int.): 368 $[M]^+$ (2.5), 263 $[M-PhCO]^+$ (2), 105 $[PhCO]^+$ (100), 77 $[C_6H_5]^+$ (34); HRMS *m*/*z* 368.1618 (calcd for $C_{22}O_5H_{24}$ 368.1624).

(6*R*),(7*S*),(11*R*)-11,13-Dibenzoyloxy-4(15),10(14)-diene-guaiane-6α,12-olide (**10**) was obtained as an amorphous white solid. ^{1}H NMR (600 MHz): see **Table 1**. *J* (Hz): 1,2α = 8.0; 1,2β = 4.0; 1,5 = 9.0; 2α, 2β = 13.6; 2α,3α = 2α,3β = 6.8; 2β,3β = 9.2; 5,6 = 6,7 = 9.6; 7,8α = 2.8; 7,8β = 12.4; 8α,8β = 12.4; 8β,9α = 12.4; 8β, 9β = 4.9; 8α,9α = 11.2; 8α,9β = 4.2; 13,13′ = 11.0; 1,15 = 3,15′ = 1.7; 1,15 = 3,15′ = 1.6; 3′,4′ = 8.8; 3′,5′ = 1.6; 4′,5′ = 7.2; 3″,4″ = 8.4; 3″, 5″ = 1.6; 4″,5″ = 7.6. ^{13}C NMR (100 MHz): see **Table 2**. EIMS (70 eV) *m*/*z* (rel. int.): 472 $[M]^+$ (0.5), 350 $[M-PhCOOH]^+$ (4), 228 $[M-2PhCOOH]^+$ (17), 105 $[PhCO]^+$ (100); HRMS *m*/*z* 472.1889 (calcd for $C_{29}O_6H_{28}$ 472.1886).

Spectroscopic Characterization: GELs. The oxidation step was optimized with 13-hydroxy-*epi*-costuslactone (**3**) to yield 13-oxo-*epi*-costuslactone **11**. With this aim in mind, several oxidizing agents were tested, and periodinane gave the best yields (57%, data not shown for other reagents). Compound **11** presented a molecular ion in the HRMS at *m*/*z* 246.12559, and this corresponds to the molecular formula $C_{15}H_{18}O_3$. The main diagnostic changes that support oxidation to the aldehyde were the shielding effect experienced by the signal of the H-13 protons (δ 3.74 ppm, 1H, *brd*, H-13′; δ 4.00 ppm, 1H, *brd*, H-13) and the C-13 carbon (δ 67.8 ppm) in **3**, which appeared now at δ 9.88 ppm (1H, *brs*, H-13) and δ 195.2 ppm, respectively, in the new compound (**11**).

The incorporation of the second lactone ring is supported by the HRMS spectrum, which presents a molecular ion at *m*/*z* 342.1483 (**13**) and *m*/*z* 342.1473 (**14**) according to the molecular formula $C_{20}O_5H_{22}$ and the new signals in the ^{1}H and ^{13}C NMR spectra corresponding to the H-2′, H-3′, and H-6′ protons on the lactone ring (**Tables 1** and **2**). Ring D is attached to the SL backbone through the oxygen atom, as shown by the position of the signals corresponding to proton H-2′ (δ 6.08 ppm, *dd*, *J* = 1.3 Hz, *J* = 1.5 Hz, **13**; δ 6.09 ppm, *dd*, *J* = 1.3 Hz, *J* = 1.5 Hz, **14**), which are similar to those of strigolactones (*23*, *40*, *41*) and 11,13-dihydro-GELs obtained previously; the shielding of the H-13 proton from the typical aldehyde position (δ 9.88 ppm, **11**) to an enol position (δ 7.43 ppm in both **13** and **14**); and the g-HMBC connection established through the oxygen bridge between the signals of H-2′ and C-13.

Table 3. Net Atomic Charges Calculated Using Semiempirical (PM3, AM1) and Ab Initio (Hartree−Fock, Basis Set 3-21G(*)) Methods for the Two Possible Stereochemical Configurations for Enolate **12**[a]

	Z enolate				*E* enolate			
	CS Draw	Spartan			CS Draw	Spartan		
	PM3	PM3	AM1	3-21G(*)	PM3	PM3	AM1	3-21G(*)
O13	−0.6317	−0.493	−0.451	−0.689	−0.6848	−0.530	−0.487	−0.732
C11	−0.5537	−0.668	−0.560	−0.551	−0.6482	−0.658	−0.556	−0.534
C13	+0.2178	+0.381	+0.270	+0.403	+0.4265	+0.382	+0.266	+0.399
O12	−0.5283	−0.460	−0.404	−0.687	−0.6535	−0.490	−0.435	−0.717
O6	−0.3909	−0.307	−0.321	−0.654	−0.3019	−0.292	−0.310	−0.649

[a] Values were calculated using the MOPAC interface included in Chem3D Ultra (v. 7.0) and Spartan'06.

Usually, the reaction between the enolate from a 1,3-dicarbonyl system and an electrophile proceeds through the carbon of the enolate. Examples of reaction through the oxygen are not uncommon, but they are rare. Molecular semiempirical (AM1, PM3) and ab initio (Hartree−Fock 3-21G(*)) calculations show that there is a significant difference of about 0.1 e^- between the electronic density at the O-13 oxygen atom and carbon C-11 in enolate **12** (**Table 3**). This difference appears in the two possible stereochemistries (*Z* and *E*) of the enolate. Such a difference alone would not explain why only the oxygen undergoes electrophilic attack, but along with the steric hindrance at C-11, this is expected to be enough to direct the reaction pathway through the oxygen and not through C-11.

Extensive NOE and NOESY studies on both diastereomers **13** and **14** did not provide any helpful positive NOE effect that could serve to discriminate between a *Z* or *E* configuration at the Δ11−13 double bond. However, the synthetic approach used here has previously been applied to obtain strigolactones (*36*, *42*) and its synthetic analogues (*43*), and the *E* enolate was obtained in all cases. The similarity between the ABC systems in guaianolides and strigolactones, where both backbones adopt a similar spatial arrangement, makes it reasonable to believe that the result should be the same in GELs (**Figure 3A**). A similar arrangement is obtained when the *E* enolate of aldehyde **11** is overlapped with strigol. Consequently, using as a working hypothesis the *E* stereoisomer at the C11−C13 double bond, an exhaustive study of the theoretical distances between H-13a and H-8β in all conformers in dehydrocostuslactone (**1**) and guaianestrigolactones **13** and **14** was performed.

The results show that in the case of the double bond with a *Z* disposition, the distance between H-13a and H-8β is almost the same in the minimum energy conformer (**Table 4**, **Figure 3B**) for all three compounds. Also, calculation of the Boltzmann distribution shows that the minimum energy conformer accounts for more than 90% of the population in each of the three compounds (**Figure 4**) and that in each local minima H-13,H-8 distances are in the range of 2.1 to 3.2 Å. The overlapping of the theoretical minimum energy conformer in **1**, (Δ11,13*Z*)-**13** and (Δ11,13*Z*)-**14**

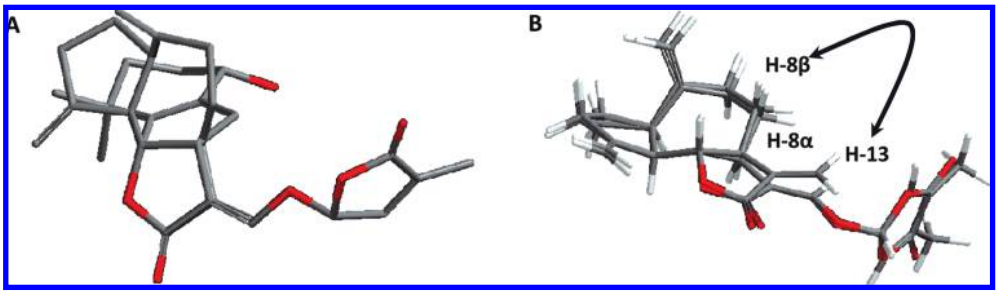

Figure 3. (**A**) Overlapping of DHC (**1**) and strigol minimum energy conformers as obtained from PM3 calculations (Spartan'06). (**B**) Overlapping of theoretical minimum energy conformers of **1**, Δ11,13(*Z*)-**13** and Δ11,13(*Z*)-**14** calculated using the MMFF force field. The arrow depicts the NOE effect observed in DHC (**1**).

also shows a similar spatial disposition for all of these species (**Figure 3B**). Irradiation of the H-13a signal gave a strong NOE effect between the signals corresponding to protons H-13a and H-8α in the case of dehydrocostuslactone (**1**). However, on irradiating either H-13 or H-8β signals no NOE effect nor, in fact, a single correlation was detected in the NOESY experiment in the case of guaianestrigolactones **13** and **14**. Consequently, even though the absence of NOE effects cannot usually be taken as evidence for the stereochemical configuration, in this case the comparison between the theoretical distances in DHC (**1**) and GELs **13** and **14** correlate well with an *E* stereoisomer of the C11−C13 double bond on the basis of the absence of any NOE effect.

Table 4. Theoretical Distances between H-13, H-8α, and H-8β as Calculated from the Minimum Energy Conformers of Compounds **1**, Δ11,13(*Z*) (**13**), and Δ11,13(*Z*) (**14**) Obtained Using PM3 and MMFF Calculations (Spartan'06)

	H13-H8α (Å)	H13-H8β (Å)
DHC (**1**)	2.33	3.19
(C2′R), Δ11−13(*Z*) (**13**)	2.29	3.17
(C2′S), Δ11−13(*Z*) (**14**)	2.30	3.13

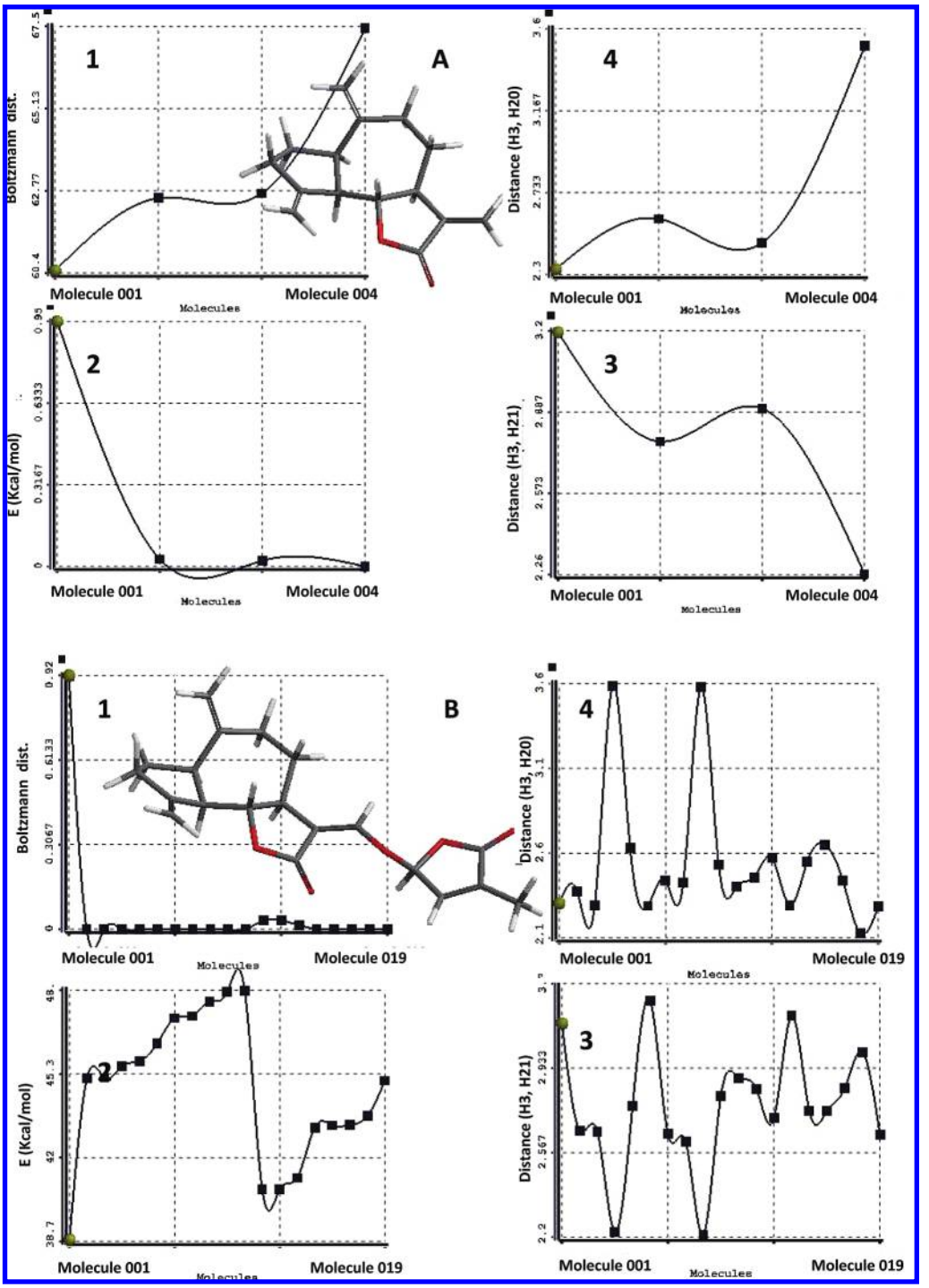

Figure 4. Comparison of the H-13-H8α and H-13-H8β distances throughout the conformer distribution of **1** (**A**) and Δ11,13(*Z*) (**14**) (**B**) as calculated using the MMFF force field from a previously PM3 minimized structure. Key: 1, Boltzmann distribution (total population normalized to 1); 2, torsion and steric energy of each conformer (kcal/mol); 3, distance between H13-H8α (Å); 4, distance between H13-H8β (Å).

The third problem to be addressed with these compounds is the issue of the configuration at C-2′. Assignment of the absolute configuration at C-2′ is a crucial issue as it has been reported that this chiral center greatly affects the germination activity on *Striga* and *Orobanche* spp. (*44*, *45*).

Frischmuth et al. developed an empirical rule to assign the absolute configuration of strigolactones based on the sign of the circular dichroism (CD) spectra above $\lambda = 270$ nm, which corresponds to the change in the arrangement at the C-2 stereocenter of Feringa's lactone (*46*). When recorded alone, each of the two possible C-2′ enantiomers (**17** and **18**, **Figure 5**) gives opposite CD spectra, and the sign above 270 nm correlates with the C-2′S (+) or C-2′R (−) configuration at this center, this being the empirical rule developed for these compounds. The basic assumption is that the whole of the CD spectra of strigolactones can be split in two as the sum of the ABC ring spectrum (**15** and **16**) (which basically contributes to the spectra below $\lambda = 250$ nm) and that of Feringa's lactone (**17** and **18**) (**Figure 5**) and that the two chromophores (the enol-lactone system and the unsaturated cyclobutanone ring) can be considered as independent. The case of GELs can be considered to be essentially the same, as they share with strigolactones the lactone−enol−γ-lactone moiety (C and D rings). The CD spectra of **13** and **14** (**Figure 6**) are similar to those of strigolactones (*46*) and show a change in the sign of the CD above $\lambda = 270$ nm. However, the CD spectrum of **11** shows that this part of the molecule contributes to the overall spectrum mainly at wavelengths below 270 nm and that its contribution beyond this value can be dismissed (**Figure 6**). Consequently, we applied Frischmuth's rule to GELs once it had been proven that both skeletons behave in a similar manner in terms of CD. The assignment of the absolute configuration at C-2′ was obtained for each enantiomer (**Table 5**) as C-2′R for GEL **13** and C-2′S for GEL **14**.

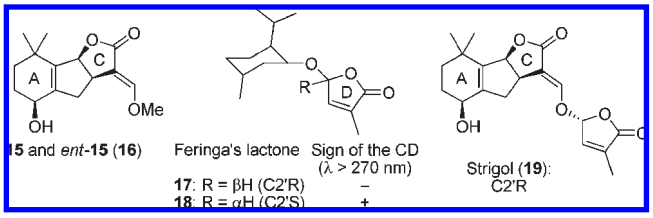

Figure 5. Feringa's lactone and ABC system of strigolactones.

(11*E*)-(2′*R*)-13-[4′-Methyl-3′-ene-2′-oxy-γ-butyrolactone]-4(15),10(14),11(13)-triene-guaiane-6α,12-olide (**13**) was obtained as a colorless oil; $[\alpha]^{25}_{D}$ +0.038 (*c* 0.04, $CHCl_3$); IR (neat, KBr) ν_{max} 2927 (C−H), 1778, 1759 (C=O, γ-lactone), 1678 (C=C) cm^{-1}. ^1H NMR (600 MHz): see **Table 1**. *J* (Hz): 1,5 = 5,6 = 9.2; 6,7 = 8.5; 7,8α = 3.3; 7,8β = 12.0; 9α,9β = 13.1; 8α,9β = 3.1; 8α,9α = 8β,9β = 5.6; 8β,9α = 9.7; 7,13 = 3.1; 3,15 = 3,15′ = 1.8; 2′,3′ = 1.5; 2′,6′ = 1.3; 3′,6′ = 1.8. ^{13}C NMR (100 MHz): see **Table 2**. EIMS (70 eV) *m*/*z* (rel. int.): 342 $[M]^+$ (2); 245 $[M-C_5H_5O_2]^+$ (20); 97 $[M-C_{15}H_{17}O_3]^+$ (100); HRMS *m*/*z* 342.1473 (calcd for $C_{20}O_5H_{22}$ 344.1479).

(11*E*)-(2′*S*)-13-[4′-Methyl-3′-ene-2′-oxy-γ-butyrolactone]-4(15),10(14),11(13)-triene-guaiane-6α,12-olide (**14**) was obtained as a colorless oil; $[\alpha]^{25}_{D}$ −0.037 (*c* 0.04, $CHCl_3$); IR (neat, KBr) ν_{max} 2927 (C−H), 1783, 1751 (C=O, γ-lactone), 1680 (C=C) cm^{-1}. ^1H NMR (600 MHz): see **Table 1**. *J* (Hz): 1,5 = 9.0; 5,6 = 10.0; 6,7 = 8.7; 7,8α = 3.6; 7,8β = 11.8; 9α,9β = 13.1; 8α,9β = 8β,9β = 5.4; 7,13 = 3.1; 3,15 = 3,15′ = 1.5; 2′,3′ = 3′,6′ = 1.5; 2′,6′ = 1.3. ^{13}C NMR (100 MHz): see **Table 2**. EIMS (70 eV) *m*/*z* (rel. int.): 342 $[M]^+$ (2); 245 $[M-C_5H_5O_2]^+$ (20); 97 $[M-C_{15}H_{17}O_3]^+$ (100); HRMS *m*/*z* 342.1483 (calcd for $C_{20}O_5H_{22}$ 344.1479).

Bioassays. Compounds **1**−**4**, **6**−**11**, and **13**−**15** were tested as germination inducers. Compound **15** is the parent 2-methylpent-2-ene-lactone, that has been included in the bioassay to test the lactone ring alone. The guaianolide backbone was selected as a target based on our previous results, which showed that eudesmanolides and melampolides presented a lower germination index (*31*). In this study, compounds were designed and synthesized to check the following hypotheses: (i) the lactone ring itself is sufficient to induce germination in *O. cumana* (sunflower broomrape); (ii) the lactone−enol−γ-lactone-like system is a more general bioactiphore; it can be generally recognized by broomrapes other than sunflower-parasitizing species; and (iii) the introduction of a second lactone ring can increase the levels of low-germination activity compounds.

Compounds **1**−**4** and **6**−**10** were tested on two different populations of *O. cumana* (IN12 and IN23) and one population of *O. ramosa*, while compounds **11**−**14** were tested only on one

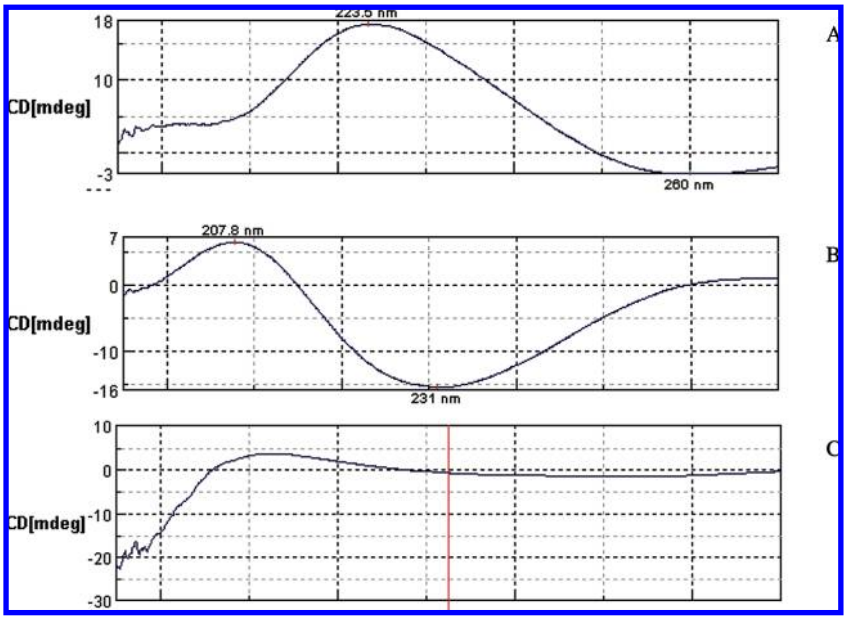

Figure 6. Comparison of CD spectra from GELs **13** (**A**) and **14** (**B**), and the aldehyde **11** (C).

Table 5. Assignment of the Stereochemical Configuration at C-2′ in GELs Based on the Change of the Sign in the CD Spectrum (*46*)

compound	C-2′ absolute configuration	Sign of CD above λ = 270 nm (260 for GELs)
Feringa's lactone **17**	*R*	−
Feringa's lactone **18**	*S*	+
strigol (**19**)	*R*	−
2′-*epi*-strigol (**20**)	*S*	+
GEL **13**	*R*	−
GEL **14**	*S*	+

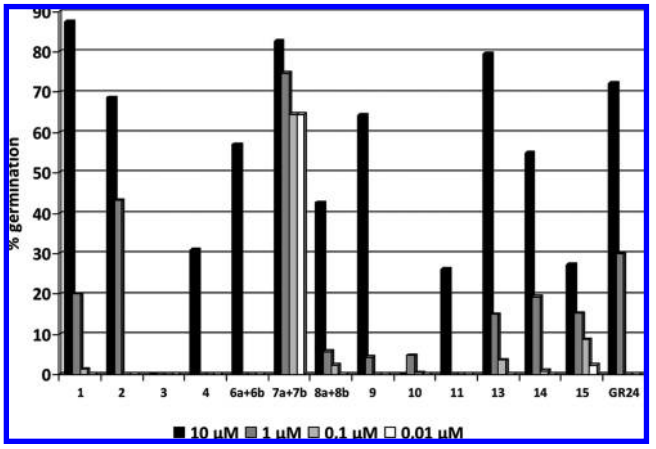

Figure 7. Effects of guaianolides **1**−**4**, **9**−**11**, γ-butirolactone **15**, dihydroGELs **6**−**8**, and GELs **13**−**14** on the germination of *Orobanche cumana* (IN23) seeds. GR24 was tested at the same concentrations as the internal standard for bioassay reproducibility.

population of *O. cumana* (IN23) and one of *O. ramosa*. Seeds of *O. cumana* IN12 showed a greater dormancy than IN23 (data not shown), and the percentages of germination obtained with GR24 and test compounds were lower. However, no differences were found in the activity profiles of compounds tested between the two populations. Consequently, the discussion will be focused on the population with the higher germination percentage (IN23). The results are shown in **Figures 7** (*O. cumana*) and **8** (*O. ramosa*) and the EC50 values in **Table 6**.

In general, all compounds induced germination of the two populations of *O. cumana* with two exceptions: the dibenzoyl derivative **10** and, interestingly, the 13-hydroxy-*epi*-costuslactone **3**. However, its epimer at C-11 (hydroxy-costuslactone **2**) remains active, thus illustrating the importance of the stereochemical configuration. It should also be noted that the γ-butyrolactone alone (**15**) was able to induce germination of *O. cumana*, albeit to a much lower extent than the other compounds or GR-24.

Major differences arose for **6**−**8**, **13**, and **14** when tested on *O. ramosa*. None of the SLs (**1**−**4** and **9**−**11**) and γ-butyrolactone **5** induced germination of tobacco broomrape, a finding that is not unexpected; in contrast, the new GELs (**13** and **14**) and dihydroGELs (**6**−**8**) proved to be active. These results are in good agreement with previous results, which showed the high selectivity of SL toward sunflower broomrape (*31*) and confirmed hypothesis ii, i.e., that the incorporation of a new lactone ring to mimic the strigolactone lactone−enol−γ-lactone system caused a loss of selectivity and made compounds active toward *O. ramosa* when they previously did not show any activity (**2**−**4** and **11**).

Regarding the molecular modeling of the compounds tested, the results for molecular properties are summarized in **Table 7**, in which the main physicochemical features linked to the discussion of the bioassays are presented.

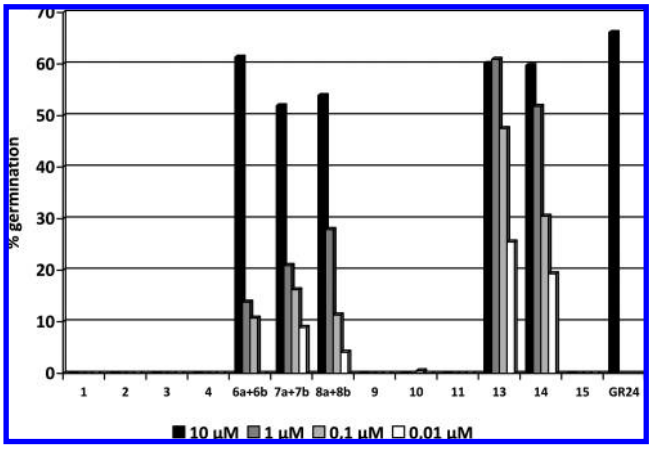

Figure 8. Effects of guaianolides **1**−**4**, **9**−**11**, γ-butirolactone **15**, dihydroGELs **6**−**8**, and GELs **13**−**14** on the germination of *Orobanche ramosa* seeds. GR24 was tested only at 10 μM as the internal standard for bioassay reproducibility.

Table 6. EC50 Values Obtained for *O. cumana* and *O. ramosa* with Guaianolides **1**−**4**, **9**−**11**, γ-Butirolactone **15**, DihydroGELs **6**−**8**, and GELs **13**−**14**

	O. cumana		*O. ramosa*	
	EC50 (μM)	r^2	EC50 (μM)	r^2
1	2.8	0.9905	n. a.	
2	3.04	0.9524	n. a.	
3	n. a.		n. a.	
4	27.5		n. a.	
6	8.4	0.9893	6.7	0.9927
7	0.003	0.8970	10.4	0.9799
8	13.7	0.9995	7.9	0.9727
9	6.4	0.9917	n. a.	
10	n.a.		n. a.	
11	28.2	0.9989	n. a.	
13	3.7	0.9927	0.006	0.8163
14	7.4	0.9935	1.03	0.8536
15	52.8[a]	0.9987	n. a.	

[a] Because of the low activity obtained with **15**, a classical approximation to estimate the EC50 value was used as follows: for 100% activity, a concentration of 1 M was supposed, where as a 10^{-12} M concentration was estimated for 0% activity.

One major observation is that **2**, **4**, **9**, and **11** present significant or good germination activities without possessing the typical lactone−enol−γ-lactone-like system of strigolactones, an observation that is in good agreement with our previous data (*30*, *31*). Moreover, the γ-butyrolactone ring alone (**5**) is also able to induce germination, albeit to a lower extent. These data confirm that the lactone ring is sufficient in its own right to induce *O. cumana* germination, according to hypothesis i, presented in the previous section. However, comparison between dehydrocostuslactone (**1**) and the rest of the SLs (**2**−**4** and **9**−**11**) shows that **1** presents a higher level of activity. Consequently, even though the lactone ring by itself seems to be sufficient to induce germination in *O. cumana*, the presence of the much more reactive α,β-unsaturated lactone ring enhances the activity. This finding is consistent with a molecular mechanism in which a bionucleophile reacts with the lactone ring. When the double bond is present, the reaction turns to a Michael addition pathway (**Figure 9A**), which is probably less demanding in terms of energy than the direct 1,2-addition to the carbonyl group in the lactone (**Figure 9B**).

Besides, the presence of the additional enol-γ-lactone system seems to enhance activity, as shown by comparison of the pairs **2** and **7(a + b)**, **3** and **6(a + b)**, **4** and **8(a + b)**, and **1** with **13** and **14**.

Table 7. Theroetical Molecular Properties from Selected Strigolactones and GELs

compound	molecular volume (Å^3)	height (Å)	E (HOMO) (eV)	E (LUMO) (eV)
strigol (**19**)	341.93	5.98	−9.82	−0.88
sorgolactone	316.70	8.94	−9.40	−1.01
solanacol	325.69	4.06	−9.39	−0.95
sorgomol	348.77	7.15	−9.81	−1.06
1 (DHC)	250.43	3.90	−9.78	−0.15
2 (13-hydroxy)	261.20	5.00	−9.86	+0.71
4 (11,13-dihydroxy)	268.94	5.18	−9.86	+0.71
5 (γ-butyrolactone)	102.94	1.80	−10.44	−0.41
11 (aldehyde)	257.40	5.03	−9.86	+0.32
9 (benzoyloxi)	376.21	5.61	−9.82	−0.45
10 (dibenzoyloxi)	482.28	15.36	−9.77	−0.51
dihydroGEL **6** (2′ R)	351.6	7.21	−9.80	−0.51
dihydroGEL **7** (2′ R)	352.4	5.98	−9.90	−0.38
dihydroGEL **8** (2′ R)	359.1	5.17	−9.90	−0.52
GEL **13** (2′ R)	347.8	7.21	−9.73	−0.91
GEL **14** (2′ S)	347.9	7.21	−9.71	−0.88

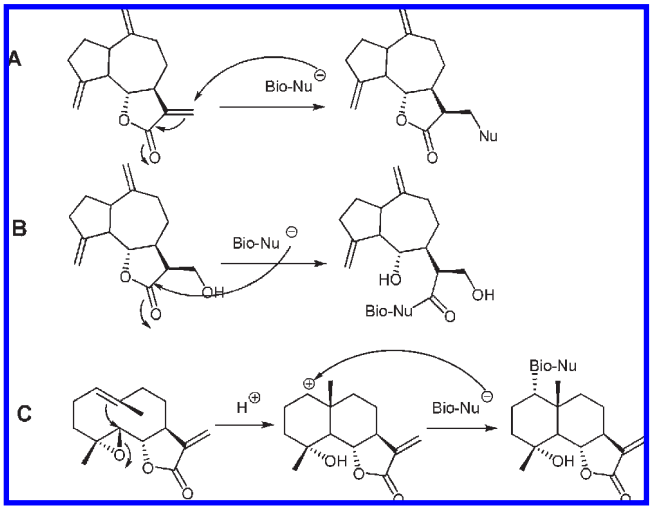

Figure 9. Possible molecular mechanisms of action for SLs under a variety of chemical environments in the lactone ring.

The germination percentages at 10 μM increase in GELs, which also induce germination at the subsequent dilutions. A clear explanation for this behavior is not obvious, but it could be due to the increased number of possible bioactiphores in these molecules (two lactone rings instead of just a single one). However, further bioassays to compare these types of pairs (lactones vs lactone−enol−γ-lactones) are necessary to confirm this hypothesis.

An important point to discuss is whether the presence of the lactone system is sufficient by itself to induce germination. It seems that other factors such as the spatial volume must also be considered. In this sense, a dramatic reduction in activity can be observed when **9** and **10** are compared. Compound **9** presents activity similar to that of its parent **4**. However, **10** is inactive. The main differences between the two compounds are their molecular volumes. We previously reported (*31*) that natural strigolactones present theoretical volumes between 290.5 and 435.6 Å^3. We calculated several theoretical molecular descriptors for this new set of compounds and found that benzoyl derivative **9** has a molecular volume of 449.5 Å^3, while dibenzoyl derivative **10** has a volume of 566.7 Å^3. GELs also present theoretical molecular volumes within the strigolactone range (**Table 7**). Initially, the lack of activity of **10** can be related to a molecular volume that is too high and should not fit into the receptor cavity. Consequently, a tentative volume for the bioactiphore could be proposed in the range 450−560 Å^3, on the basis of the largest volume of an active compound (**9**) and the lowest volume of an inactive compound (**10**). However, this assumption proved to be questionable in view of data obtained later with another set of compounds (data not shown) in which GELs with volumes greater than that of **10** showed reasonable to excellent levels of activity. The lack of activity seems to be related with the spatial requirements of the 11,13-dibenzoyl system rather than with the overall volume of the molecule. The minimum energy conformer adopted by **10** to minimize the steric hindrance caused by the two bulky aromatic rings (**Figure 9**) gives a distance between the two extremes (that could be considered as the height of the molecule) of 15.36 Å, a value far higher than those characteristic of strigol (5.98 Å), dihydroGEL **8** (7.2 Å), or GEL **14** (7.21 Å; total height 8.4 Å). As a consequence, it seems that the lack of activity of **10** must be due to steric reasons rather than with the functional groups present in ring C, in this particular case (**Figure 10**), as it will not fit the spatial requirements of the receptor cavity.

Another point worth highlighting concerns **3**. Previous results with populations IN7 and IN21 of *O. cumana* (*31*) showed this compound to be extremely active. However, it turned now to be inactive with populations IN12 and IN23. The bioassay was repeated three times in order to ensure the accuracy of the results. This fact might be understood as a signal of the high genetic variability of *Orobanche* that might change specific recognition requirements from one population to another, making it sometimes difficult to correlate results from different populations.

Finally, the third key point in discussion addresses the question of the bioactiphore and whether the lactone−enol−γ-lactone system of strigolactones is a general recognition system for all *Orobanche* species or whether there are other groups that can be also recognized. Comparison of germination activities of *O. cumana* and *O. ramosa* clearly show that SLs are specific inducers of *O. cumana* germination. However, when a second lactone ring is added to the guaianolide skeleton in a strigolactone fashion (rings C and D, GELs), the selectivity of SL toward *O. cumana* disappears, and the resulting compounds (**6**−**8**, **13**, **14**) now induce germination in other *Orobanche* species, tobacco broomrape in this case. Consequently, it is reasonable to propose that the lactone ring is the specific bioactiphore for *O. cumana*, and a more general system that can be recognized by all Orobanchaceae corresponds to the lactone−enol−γ-lactone system. As a consequence, the proposed hypothesis that SLs are the specific sunflower allelochemicals that trigger germination in *O. cumana* is strongly supported by these data. SLs are common constituents of sunflowers, and if exuded from the roots of sunflowers, they

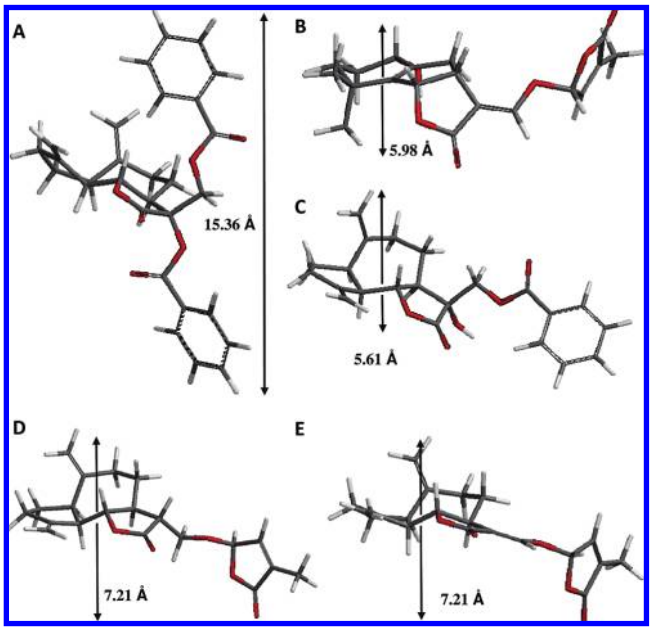

Figure 10. Distance between the bottom and roof of (**A**) 11,13-dibenzoyloxy-DHC (**10**); (**B**) strigol; (**C**) 11-hydroxy-13-benzoyloxy-DHC (**9**); (**D**) 2′S-dihydroGEL (**7**); and (**E**) 2′S-GEL (**14**) as obtained from the minimum energy conformer calculated using semiempirical PM3 calculations (Spartan'06).

could be the specific host signals that induce germination of sunflower broomrape seeds.

Regarding the molecular recognition mechanism, a nucleophilic Michael addition of the nucleophile present in the receptor's cavity followed by a retro-Michael reaction has been proposed (*47*). In the case of SLs, several mechanisms could be proposed to explain activity, even when the exocyclic double bond conjugated with the lactone system is not present (**Figure 9**) (*48*).

Entry a represents the most general situation. The bionucleophile reacts in a Michael fashion and becomes bound irreversibly to the SL. The end product is similar to that proposed by Zwanenburg for strigolactones. Entry b represents those cases where the exocyclic double bond is not present, and a Michael addition of the bionucleophile is not possible. In these cases, the lactone ring itself may undergo a nucleophilic addition that leads to the opening of the lactone ring. The steric constraints are higher, and the reactivity of the lactone ring is lower in this case, thus explaining the lower activities obtained with the reduced SLs in comparison with their unsaturated analogues. According to this model, the nucleophilic addition involves the reaction of the HOMO from the bionucleophile with the LUMO of the guaianolide, strigolactones, or GEL. When the double bond is not present in the lactone ring (**2**−**4** and **11**), the energy of the LUMO rises up as a result of the lower reactivity of these compounds (**Table 7**, compounds **2**, **4**, and **11**), which can be also correlated with their lower germination indexes. This is not the case of **9**, which lacks the double bond at the lactone ring but presents a high germination index and energy of the LUMO similar to dihydroGELs (**6**−**9**). The presence of the aromatic benzoyl group lowers the energy LUMO and may change the reactivity of the molecule as it is a good leaving group that can undergo SN_2 displacements. This fact, plus their location in the reactive bioactiphore zone of the SL might serve to explain its high bioactivity.

Entry c represents a third possibility in which other nucleophilic reaction centers are present in the molecule. Germacranes readily react under acidic conditions to give rise to eudesmanolides (*49*, *50*). Physiological pH values are mildly acidic, and reactions such as those depicted in entry c are possible. Thus, the previously reported order of reactivity parthenolide > reduced parthenolide (*31*) is explained.

The accepted ecological role of SLs in sunflowers (and in other plant species where they are present) is chemical defense against insects and aphids, fungi, and competing plants. In order to act as chemical clues for parasitic weeds, SLs should be exuded through the roots or leached from the leaves by rain into the soil. However, such studies have not been carried out with sunflower exudates to date nor has the presence of SLs outside the plant been confirmed. In the absence of such data, our preliminary results strongly support the hypothesis that SLs exuded through the roots of sunflowers are the specific inducers of the germination of sunflower broomrape. Broomrape might coevolve with sunflowers in order to take advantage of this defense mechanism, changing it into a clear signal that a host is available in the vicinity of the seed.

Supporting Information Available: Discussion on the stereoselectivity of the SN2 displacement of bromine to yield **6a** + **6b**, **7a** + **7b**, and **8a** + **8b** based on theoretical calculations, molecular mechanics, *semi*-empirical (AM1 and PM3), ab initio (Hartree−Fock), and denstity functional (B3LYP); molecular calculations supporting the stereochemical configuration proposed at the double bond C11−C13 in GELs **13** and **14**; and ^{1}H and ^{13}C NMR spectra of all new compounds **6a** + **6b**, **7a** + **7b**, and **8a** + **8b**, **9**−**14**. This material is available free of charge via the Internet at http://pubs.acs.org.

LITERATURE CITED

(1) Joel, D. M.; Hershenhorn, Y.; Eizenberg, H.; Aly, R.; Ejeta, G.; Rich, P. J.; Ransom, J. K.; Sauerborn, J.; Rubiales, D. Biology and management of weedy root parasites. *Hort. Rev.* **2007**, *33*, 267–349.

(2) Cubero, J. I. Parasitic Diseases in *Vicia faba* L. with Special Reference to Broomrape (*Orobanche crenata* Forsk.). In *The Faba Bean*; Hebblethwaite, P. D., Ed.; Butterworths: Oxford, U.K., 1982; pp 496−521.

(3) Nandula, V. K.; Westwood, J. H.; Foster, J. G.; Foy, C. L. Influence of glyphosate on amino acid composition of Egyptian broomrape [*Orobanche aegyptiaca* (Pers.)] and selected hosts. *J. Agric. Food Chem.* **2001**, *49*, 1524–1528.

(4) Castejón-Muñoz, M.; Romero-Muñoz, F.; García-Torres, L. Control of broomrape (*Orobanche cernua*) in sunflower (*Helianthus annuus* L.) with glyphosate. *Crop Prot.* **1990**, *9*, 332–336.

(5) Qasem, J. R. Chemical control of branched broomrape (*O. ramosa*) in glasshouse grown tomato. *Crop Prot.* **1998**, *17*, 625–630.

(6) Eizenberg, H.; Hershenhorn, J.; Graph, S.; Manor, H. *Orobanche aegyptiaca* control in tomato with sulfonylurea herbicides. *Acta Hort.* **2003**, *613*, 205−208.

(7) Schnell, H.; Kunisch, M.; Saxena, M. C.; Sauerborn, J. Simulation of the seed bank dynamics of *Orobanche crenata* Forsk. in some crop rotations common in Northern Syria. *Exp. Agric.* **1996**, *32*, 395–403.

(8) Fernández-Aparicio, M.; Sillero, J. C.; Rubiales, D. Intercropping with cereals reduces infection by *Orobanche crenata* in legumes. *Crop Prot.* **2007**, *26*, 1166–1172.

(9) Jain, R.; Foy, C. L. Nutrient effect on parasitism and germination of egyptian broomrape (*Orobanche aegyptiaca*). *Weed Technol.* **1992**, *6*, 269–275.

(10) Roman, B.; Torres, A. M.; Rubiales, D.; Cubero, J. I.; Satovic, Z. Mapping of quantitative trait loci controlling broomrape (*Orobanche crenata* Forsk.) resistance in faba bean (*Vicia faba* L.). *Genome* **2002**, *45*, 1057–1063.

(11) Pérez-de-Luque, A.; Jorrin, J. V.; Rubiales, D. Crenate broomrape control in pea by foliar application of benzothiadiazole (BTH). *Phytoparasitica* **2004**, *32*, 21–29.

(12) Echevarría-Zomeño, S.; Pérez-de-Luque, A.; Jorrín, J.; Maldonado, A. M. Pre-haustorial resistance to broomrape (*Orobanche cumana*) in sunflower (*Helianthus annuus*): cytochemical studies. *J. Exp. Bot.* **2006**, *57*, 4189–4200.

(13) Perez-Vich, B.; Akhtouch, B.; Knapp, S. J.; Leon, A. J.; Velasco, L.; Fernandez-Martinez, J. M.; Berry, S. T. Quantitative trait loci for broomrape (*Orobanche cumana* Wallr.) resistance in sunflower. *Theor. Appl. Genet.* **2004**, *109*, 92–102.
(14) Rubiales, D. Parasitic plants, wild relatives and the nature of resistance. *New Phytol.* **2003**, *160*, 459–461.
(15) Johnson, A. W.; Gowda, G.; Hassanali, A.; Knox, J.; Monaco, S.; Razavi, Z.; Rosebery, G. The preparation of synthetic analogs of strigol. *J. Chem. Soc., Perkin Trans.1* **1981**, *6*, 1634–1743.
(16) Galindo, J. C. G.; Macías, F. A.; García-Díaz, M. D.; Jorrín, J. Chemistry of Host-Parasite Interactions. In *Allelopathy. Chemistry and Mode of Action of Allelochemicals*; Macías, F. A., Galindo, J. C. G., Molinillo, J. M. G., Cutler, H. G., Eds.; CRC Press: Boca Raton, FL, 2004; pp 125−148.
(17) Rani, K.; Zwanenburg, B.; Sugimoto, Y.; Yoneyama, K.; Bouwmeester, H. J. Biosynthetic considerations could assist the structure elucidation of host plant produced rhizosphere signaling compounds (strigolactones) for arbuscular mycorrhizal fungi and parasitic plants. *Plant Physiol. Biochem.* **2008**, *46*, 617–626.
(18) Siame, B. A.; Weerasuriya, Y.; Wood, K.; Ejeta, G.; Butler, L. G. Isolation of strigol, a germination stimulant for *Striga asiatica*, from host plants. *J. Agric. Food Chem.* **1993**, *41*, 1486–1491.
(19) Hauck, C.; Müller, S.; Schildknecht, H. A germination stimulant for parasitic flowering plants from *Sorghum bicolor*, a genuine host plant. *J. Plant Physiol.* **1992**, *139*, 474–478.
(20) Yoneyama, K.; Sato, D.; Takeuchi, Y.; Sekimoto, H.; Yokota, T. Search for Germination Stimulants and Inhibitors for Root Parasitic Plants. Abstracts of Papers, 227th National Meeting of the American Chemical Society, Anaheim, CA; American Chemical Society: Washington, DC, 2004.
(21) Yokota, T.; Sakai, H.; Okuno, K.; Yoneyama, K.; Takeuchi, Y. Alectrol and Orobanchol, germination stimulants for *Orobanche minor*, from its host red clover. *Phytochemistry* **1998**, *49*, 1967–1973.
(22) Müller, S.; Hauck, C.; Schildknecht, H. Germination stimulants produced by *Vigna unguiculata* Walp cv. Saunders. *J. Plant Growth Reg.* **1992**, *11*, 77–84.
(23) Cook, C. E.; Whichard, L. P.; Thurner, B.; Wall, M. E.; Egley, G. H. Germination of witchweed (*Striga lutea* Lour.): isolation and properties of a potent stimulant. *Science* **1966**, *154*, 1189–1190.
(24) Yasuda, N.; Sugimoto, Y.; Kato, M.; Inanaga, S.; Yoneyama, K. (+)-Strigol, a witchweed germination stimulant from *Menispermum dauricum* root culture. *Phytochemistry* **2003**, *62*, 1115–1119.
(25) Akiyama, K.; Matsuzaki, K.-I.; Hayashi, H. Plant sesquiterpenes induce hyphal branching in arbuscular mycorrhizal fungi. *Nature* **2005**, *435*, 824–827.
(26) Akiyama, K.; Hayashi, H. Strigolactones: chemical signals for fungal symbionts and parasitic weeds in plant roots. *Ann. Bot.* **2006**, *97*, 925–931.
(27) Joel, D. M.; Steffens, J. C.; Matthews, D. E. Germination of Weedy Root Parasites. In *Seed Development and Germination*; Kigel, J., Galili, G., Eds.; Marcel Dekker: New York, 1995; pp 567−597.
(28) Bar Nun, N.; Mayer, A. M. Preconditioning and germination of *Orobanche* seeds: respiration and protein synthesis. *Phytochemistry* **1993**, *34*, 39–45.
(29) Bar Nun, N.; Plakhine, D.; Joel, D. M.; Mayer, A. M. Changes in the activity of the alternative oxidase in *Orobanche* seeds during conditioning and their possible physiological function. *Phytochemistry* **2003**, *64*, 235–241.
(30) Pérez de Luque, A.; Galindo, J. C. G.; Macías, F. A.; Jorrín, J. Sunflower sesquiterpene lactone models induce *Orobanche cumana* seed germination. *Phytochemistry* **2000**, *53*, 45–50.
(31) Galindo, J. C. G.; de Luque, A. P.; Jorrín, J.; Macías, F. A. SAR studies of sesquiterpene lactones as *Orobanche cumana* seed germination stimulants. *J. Agric. Food Chem.* **2002**, *50*, 1911–1917.
(32) Mathur, S. B.; Hiremath, S. V.; Kulkarni, G. H.; Kelkar, G. R.; Bhattacharyya, S. C.; Simonovic, D.; Rao, A. S. Terpenoids. LXX. Structure of dehydrocostus lactone. *Tetrahedron* **1965**, *21*, 3575–3590.
(33) Da Silva, A. J. R.; García, M.; Baker, P. M.; Rabi, J. A. Carbon-13 NMR spectra of natural products. 1. Guaianolides. *Org. Magn. Reson.* **1981**, *16*, 230–233.
(34) Humprehy, A. J.; Gaslter, A. M.; Beale, M. H. Strigolactones in chemical ecology: waste products or vital allelochemicals? *Nat. Prod. Rep.* **2006**, *23*, 592–614.
(35) Macías, F. A.; García-Díaz, M. D.; Massanet, G. M.; Gómez-Madero, J. F.; Fronczek, F.; Galindo, J. C. G. An easy access to bioactive 13-hydroxylated and 11,13-dihydroxylated sesquiterpene lactones (SL) through Michael addition of a nucleophilic hydroxyl group. *Tetrahedron* **2008**, *64*, 10996–11006.
(36) McAlpine, G. A.; Raphael, R. S.; Shaw, A.; Taylor, A. W.; Wild, H. J. Synthesis of the germination stimulant (±)-strigol. *J. Chem. Soc., Perkin Trans. 1* **1976**, 410–416.
(37) Serghini, K.; Perez , A.; Castejón-Muñoz, M.; García-Torres, L.; Jorrín, J. Sunflower response to broomrape parasitism: induced synthesis and excretion of 7-hydroxylated simple coumarins. *J. Exp. Bot.* **2001**, *52*, 2227–2234.
(38) *Spartan'06*; Wavefunction Inc.: Irvine, CA.
(39) Stewart, J. J. P. *MOPAC2007*, version 7.276w; Stewart Computational Chemistry: Colorado Springs, CO; http://OpenMOPAC.net. (accessed Nov, **2008**).
(40) Hauck, C.; Müller, S.; Schildknecht, H. A germination stimulant for parasitic flowering plants from *Sorghum bicolor*, a genuine host plant. *J. Plant Physiol.* **1992**, *139*, 474–478.
(41) Yokota, T.; Sakai, H.; Okuno, K.; Yoneyama, K.; Takeuchi, Y. Alectrol and orobanchol, germination stimulants for *Orobanche minor*, from its host red clover. *Phytochemistry* **1998**, *49*, 1967–1973.
(42) Mori, K.; Matsui, J.; Bando, M.; Kido, M.; Takeuchi, Y. Synthesis and biological evaluation of the four racemic stereoisomers of the structure proposed for sorgolactone, the germination stimulant of *Sorghum bicolor*. *Tetrahedron Lett.* **1997**, *38*, 2507–2510.
(43) Mangnus, E. M.; Jan Dommerholt, F.; de Jong, R. L. P.; Zwanenburg, B. Improved synthesis of strigol analogue GR24 and evaluation of the biological activity of its diastereomers. *J. Agric. Food Chem.* **1992**, *40*, 1230–1235.
(44) Bergmann, C.; Wegmann, K.; Frischmuth, K.; Samson, E.; Kranz, A.; Weigelt, D.; Koll, P.; Welzel, P. Stimulation of *Orobanche crenata* seed germination by (+)-strigol and structural analogues. Dependence on constitution and configuration of the germination stimulants. *J. Plant Physiol.* **1993**, *142*, 338–342.
(45) Mangnus, E. M.; Zwanenburg, B. Synthesis, structural characterization, and biological evaluation of all four enantiomers of strigol analogue GR7. *J. Agric. Food Chem.* **1992**, *40*, 697–700.
(46) Frischmuth, K.; Wagner, U.; Samson, E.; Weigelt, D.; Koll, P.; Meuer, H.; Sheldrick, W. S.; Welzel, P. Configurational assignment at C-2′ of some strigol analogues. *Tetrahedron: Asymmetry* **1993**, *4*, 351–360.
(47) Mangnus, E. M.; Zwanenburg, B. Tentative molecular mechanism of the germination stimulation of *Striga* and *Orobanche* seeds by strigol and its synthetic analogues. *J. Agric. Food Chem.* **1992**, *40*, 1066–1070.
(48) Galindo, J. C. G.; Hernández, A.; Dayan, F. E.; Tellez, M. R.; Macías, F. A.; Paul, R. N.; Duke, S. O. Dehydrozaluzanin C, a natural sesquiterpenolide, causes rapid plasma membrane leakage. *Phytochemistry* **1999**, *52*, 805–813.
(49) Jain, T. C.; McCloskey, J. E. Carbocyclization in natural products. I. Amberlite IR-210 catalyzed cyclization of costunolide. *Tetrahedron* **1975**, *31*, 2211–2214.
(50) Azarken, R.; Guerra, F. M.; Moreno-Dorado, F. J.; Jorge, Z. D.; Massanet, G. M. Substituent effects in the transannular cyclization of germacranes. Synthesis of 6-*epi*-costunolide and five steiractinolides. *Tetrahedron* **2008**, *64*, 10896–10905.

Received March 13, 2009. Revised manuscript received May 13, 2009. Accepted May 13, 2009. This research was supported by Ministerio de Ciencia y Tecnología, Spain (MCYT; Project No. AGL2005-05190).